Journal of Nuclear Materials 377 (2008) 101–108

Contents lists available at ScienceDirect

Journal of Nuclear Materials

journal homepage: www.elsevier.com/locate/jnucmat

Behavior of ferritic/martensitic steels after n-irradiation at 200 and 300 °C

M. Matijasevic, E. Lucon, A. Almazouzi *

SCK-CEN, Institute of Nuclear Materials Science, Boeretang 200, 2400 Mol, Belgium

A B S T R A C T

High chromium ferritic/martensitic (F/M) steels are considered as the most promising structural materials for accelerator driven systems (ADS). One drawback that needs to be quantified is the significant hardening and embrittlement caused by neutron irradiation at low temperatures with production of spallation elements. In this paper irradiation effects on the mechanical properties of F/M steels have been studied and comparisons are provided between two ferritic/martensitic steels, namely T91 and EUROFER97. Both materials have been irradiated in the BR2 reactor of SCK-CEN/Mol at 300 °C up to doses ranging from 0.06 to 1.5 dpa. Tensile tests results obtained between −160 °C and 300 °C clearly show irradiation hardening (increase of yield and ultimate tensile strengths), as well as reduction of uniform and total elongation. Irradiation effects for EUROFER97 starting from 0.6 dpa are more pronounced compared to T91, showing a significant decrease in work hardening. The results are compared to our latest data that were obtained within a previous program (SPIRE), where T91 had also been irradiated in BR2 at 200 °C (up to 2.6 dpa), and tested between −170 °C and 300 °C. Irradiation effects at lower irradiation temperatures are more significant.

1. Introduction

Fusion and Accelerator Driven systems are considered to have high potential for a sustainable and clean energy production in the future. In both applications, the structural materials will be exposed to particularly severe neutron radiation in addition to other environmental factors – far more severe than for current LWR (light water reactor) nuclear power plants. Neutron irradiation induces microstructural changes and degradation of the mechanical properties, especially when additional nuclear transmutations occur by high energy neutrons, such as H and He production [1].

The candidate materials should fulfill challenging requirements, such as high thermal conductivity and heat resistance, low thermal expansion, low ductile to brittle transition temperature shift, DBTT, sufficient strength with limited loss of ductility and toughness, low swelling rate, high creep resistance and good corrosion resistance [1,2], in addition to reproducible fabricability, workability and weldability.

High chromium ferritic/martensitic (F/M) steels are considered as the most promising structural materials for both fusion reactors [3] and accelerator driven systems (ADS) [2]. This type of steel has been the subject of considerable interest in the last century. In the 1950s, 9–12Cr transformable steels with low carbon (max 0.1%) have been developed for their high creep-rupture strengths combined with good oxidation and corrosion resistance at elevated temperatures and were successfully used in several industries (e.g. petroleum, aerospace, electrical power plants,...). In the 1980s, ferritic/martensitic steels have been further developed and used for fast breeder reactor core components, because of their superior resistance to irradiation damage and appropriate strength properties [4]. In recent years, martensitic steels with 9–12 wt% Cr are considered to be very promising candidates for internal structures of fusion reactors or high temperature fission reactors for their resistance to swelling and favorable mechanical properties like impact, tensile and creep resistance [5].

The selection of F/M steels is based mainly on their mechanical performance based on Charpy and/or tensile testing after irradiation in fast neutron flux irradiation facilities such as FFTF [6], PHENIX [7], BOR60 [8] at temperatures higher than 350 °C. It is anticipated that this class of steels would exhibit much more hardening and therefore embrittlement after irradiation at lower temperatures [9].

This paper reports on the results that have been accumulated at SCK-CEN on the performance of several ferritic/martensitic steels after irradiation in the Belgian Reactor 2 (BR2), at rather low temperatures and doses up to 4.5 dpa. The assessment of their post irradiation behaviour is based on their characterisation using mechanical testing methods such as fracture toughness and tensile tests. The first section describes the materials used, the irradiations and the tests performed. The second section is devoted to the detailed analysis of the materials before irradiation. Finally, the last section summarises the results obtained on the materials after post irradiation examination. The following issues are discussed: (i) the applicability of the test methods to this class of steels, (ii) the

* Corresponding author. Tel.: +32 14 33 30 96; fax: +32 14 32 12 16.
E-mail address: aalmazou@sckcen.be (A. Almazouzi).

0022-3115/$ - see front matter © 2008 Elsevier B.V. All rights reserved.
doi:10.1016/j.jnucmat.2008.02.063

Table 1
Chemical composition of T91 and EUROFER97 (wt%)

Steel	C	Cr	Mo	W	Nb	Ta	V	P	Mn	Ni	B	N	Si
T91	0.1	8.32	0.96	<0.01	0.06	~	0.24	0.02	0.43	0.24	<0.0005	0.03	0.32
E97	0.12	8.96	<0.001	1.1	<0.001	0.13	0.19	<0.005	0.43	0.007	<0.001	0.016	0.07

difference between a conventional steel (T91) and an experimental steel (EUROFER97), (iii) the effect of temperature on hardening and embrittlement.

2. Experimental

Both materials investigated are 9 Cr ferritic/martensitic steels. The first one is the commercially available ferritic/martensitic steel T91(9Cr 1MoVNb) while the second is the European Reduced Activation Ferritic Martensitic (RAFM) steel EUROFER97 (9Cr1WVTa), thereafter indicated as EUROFER97. EUROFER97 was delivered to SCK-CEN from FZK (Germany) and the T91 from CEA/Saclay (France). It should be noted that EUROFER97 was delivered in the form of a forged bar with 100 mm diameter while T91 was delivered as plates of 25 mm thickness. The samples have been used in normalized and tempered conditions. For T91, the normalizing treatment consisted of heating the alloy up to 1040 °C, holding for 1 h and then air cooling to room temperature. This treatment produced a fully martensitic structure. The tempering treatment consisted in heating the normalized steel up to 730 °C, holding for 3 h and 42 min and then air cooling to room temperature. On the other hand, the investigated samples of EUROFER97 were treated for one hour and 51 min at 979 °C, followed by air cooling before a tempering treatment at 739 °C for 3 h 42 min.

Table 2
Irradiation campaigns, number of reactor cycles, dose and temperature of irradiation for the investigated materials

Material	Irradiation	Cycles	Dose (dpa)	Temperature(°C)
E97	IRFUMA I	1	0.3	300
E97	IRFUMA II	4	1	300
E97	IRFUMA III	4 + 5	2	300
E97	IRFUMA IV	7	1.75	300
E97	IRFUMA V	4	2	300
E97	IRFUMA VI	5	2.5	300
E97 and T91	MIRE Cr	8	0.06; 0.6; 1.5	300
HT9	IRMAS	5		300
T91	SPIRE	12	2.95 and 4.36	200

The chemical composition of the steels is listed in Table 1. It can be seen that the main difference between T91 and EUROFER97 is that Mo has been replaced by W in EUROFER97 as the main solution hardener and to reduce neutron activation. Nb is added to T91 as a strong, high-temperature carbide former, and has been replaced by Ta in EUROFER97 to stabilise grain size, to improve

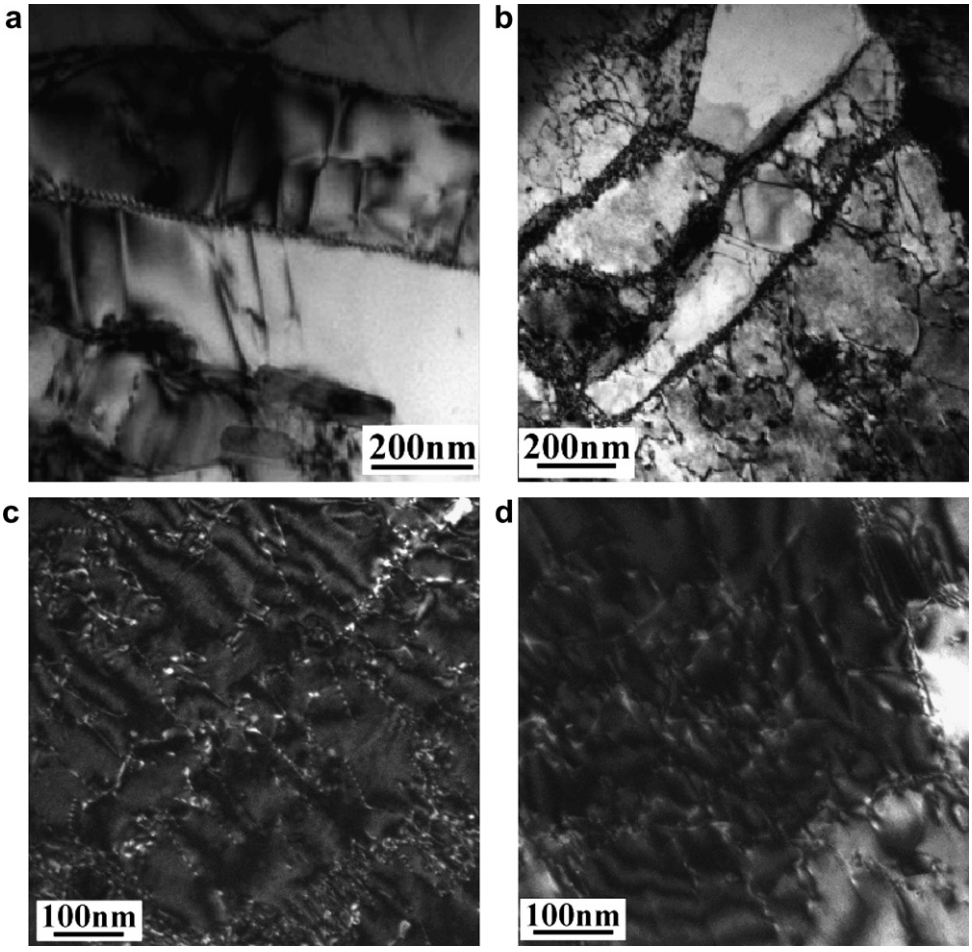

Fig. 1. Transmission electron micrographs of: (a) T91 and (b) EUROFER97 and dark field images with dislocation structure of (c) T91 and (d) EUROFER97.

the ductile to brittle transition temperature (DBTT) and strength, and to reduce neutron activation. Moreover, Ni leads to long lived isotopes and therefore has been eliminated in EUROFER97. Nevertheless, both compositions can yield a fully martensitic structure after an appropriate thermo-mechanical treatment. In fact, using the empirical equation proposed by Patriarca et al. [10] to calculate the Cr-equivalent and Ni-equivalent contained in these steels, it appears that they will be situated fully within the martensitic domain of the Schaeffler–Schneider diagram [11].

Tensile tests were performed using an electro-mechanical testing machine (INSTRON 8500, model 1362), at a strain rate of $\dot{\epsilon} = 10^{-4}\ s^{-1}$ equipped with a 10 kN load cell. The specimens were heated inside a split three-zone furnace to test the materials at elevated temperatures. The temperatures were controlled within approximately 2 °C. Tensile specimens of T91 and EUROFER97 of cylindrical cross section with overall length = 27 mm, gage length = 12 mm and diameter = 2.4 mm, were tested at temperatures from −150 °C to 300 °C, according to the ASTM E8M standard. No extensometer was used for measuring specimen elongation. Yield strength ($\sigma_{p0.2}$), ultimate tensile strength (σ_{uts}), uniform (ε_u) and total elongation (ε_t) were determined from the recorded stress–strain curves. Reduction of area (Z) was measured from the broken test pieces.

Charpy impact tests were performed on a TONI–MFL pendulum equipped with a DIN type striker (2 mm radius striker), with an impact velocity of 5.42 m/s. The sub-size Charpy-V specimens (KLST type), have the following nominal dimensions: overall length = 27 mm, thickness = 3 mm, width = 4 mm, notch depth = 1 mm. Tests were performed at temperatures from −110 °C to 300 °C. Charpy specimens of T91 and EUROFER97 were tested according to the ASTM E23 standard. The lower shelf energy E_{LSE}, the upper shelf energy E_{USE} and the DBTT were calculated from transition curves obtained by fitting a hyperbolic function (Eq. (1)) to the data.

$$E(\mathrm{J}) = \left(\frac{E_{LSE} + E_{USE}}{2}\right) + \left(\frac{E_{LSE} - E_{USE}}{2}\right)\tanh\left(\frac{T - \mathrm{DBTT}}{r}\right), \qquad (1)$$

where $E(J)$ is the impact energy, T the test temperature and r a fitting parameter related to the slope of the transition (steepness of the curve).

Precracked KLST specimens (thickness 3 mm, width 4 mm and length 27 mm) have been tested in three-point bend mode in order to determine the fracture toughness of the investigated steels in the ductile to brittle transition regime. The Master Curve approach has been applied according to the ASTM E1921-05 standard, obtaining the value of the reference temperature T_o, which corresponds to a median toughness of 100 MPa$\sqrt{m}$ for 1TCT specimens. This temperature can be used as an alternative to the Charpy-based DBTT. Tests have been carried out in displacement control, using a speed of 0.2 mm/min; load-line displacement was not measured directly, but inferred from machine crosshead displacement, accounting for the compliance of the test setup.

The samples of T91 and EUROFER97 were irradiated in the BR2 Test Reactor in Mol, during several irradiation campaigns. All irradiation experiments performed at 300 °C were performed in the CALLISTO loop [12] while those at 200 °C, were performed in a specially designed radiation rig (MISTRAL) [13]. During irradiation, the temperature of the specimens was continuously monitored within ±5 °C using thermocouples that were placed inside the irradiation capsules and very close to the specimens. The total fluence was measured with the help of dosimeters of various types that were loaded and unloaded together with the specimens. In Table 2, the different irradiation campaigns are listed with their respective temperature, number of reactor cycles and materials. Note that in the MIRE-Cr campaign the two investigated materials were irradiated under exactly the same conditions to allow a direct comparison.

3. Microstructure and mechanical properties before irradiation

T91 and EUROFER97 have both a tempered ferritic/martensitic microstructure with high dislocation density sub-boundaries in the matrix, as can be seen in the transmission electron microscope (TEM) viewgraphs a and b of Fig. 1. The photographs c and d of the same figure show the dislocation structure for T91 and E97, respectively. There are no significant differences in the martensitic lath structure and distribution of carbides between these two steels. Carbides of type $M_{23}C_6$ were found on both the grain and sub-grain boundaries. The size of the carbides varied from about 0.14–0.6 μm. The sub-boundaries are stabilized by the precipitation of carbides. Carbides also precipitate at the prior austenite grain boundaries. Dislocations have Burgers vectors of $b = a/2\ (11\bar{1})$. The dislocation density correspond to those inside the laths and they were calculated to be about $5 \times 10^9\ cm^{-2}$ for T91, while it is about $8 \times 10^9\ cm^{-2}$ for EUROFER97.

The temperature dependence of the 0.2% yield stress and the ultimate tensile strength for the two investigated steels are shown in Fig. 2(a). As can be seen on the graph, the strength decreases with increasing temperature. T91 and E97 are quite similar in this respect as they have similar yield stress and ultimate tensile strength. At room temperature the yield stress varies between 544 MPa for T91 and 557 MPa for EUROFER97 while the ultimate tensile strength varies between 684 MPa for T91 and 670 MPa for EUROFER97. At higher temperatures the difference between the ultimate tensile strength and the yield strength becomes smaller because of the loss of strain hardening capacity.

The fracture elongation measured from the broken test specimens and the uniform elongation are plotted versus the temperature in Fig. 2(b). From the graph it is shown that the elongation is always higher for T91 than for EUROFER97. This is basically the

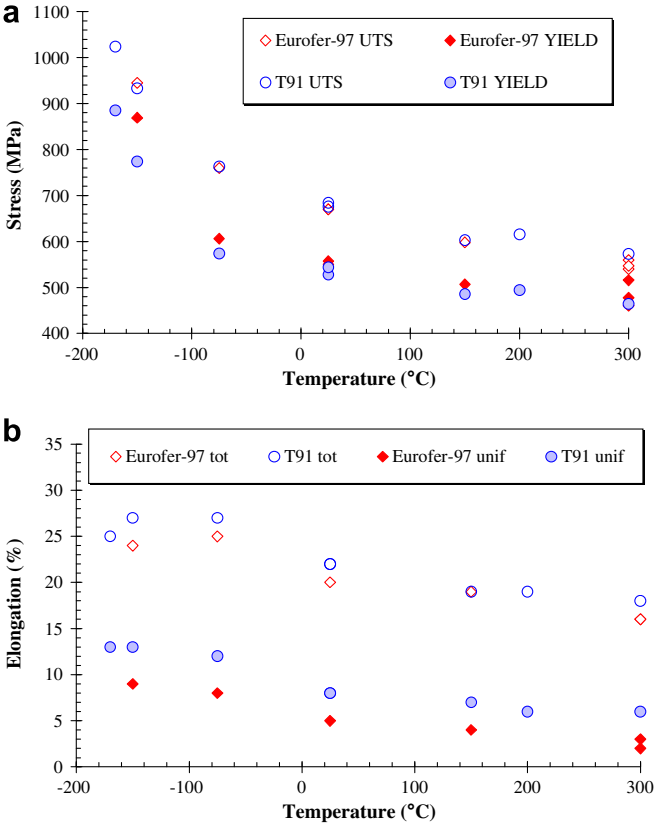

Fig. 2. Yield and ultimate tensile strengths versus temperature (top) and elongations versus temperature (bottom) for T91 and E97.

main difference between these two steels, which might be due to factors such as prior austenite grain size promoted by the presence of Ni in T91, dislocation density and structure, or carbide size and distribution. At higher temperatures, necking continues accompanied with a high reduction of area and the uniform elongation decreases more or less linearly with increasing temperature.

From impact test results and using Eq. (1), the upper shelf energy E_{USE} and the DBTT were determined. It has been observed that the transition from brittle to ductile fracture behavior appears much more abrupt for EUROFER97 than for T91, and the DBTT is also about 13 °C lower for EUROFER97 than for T91 as listed in Table 3. The shear fracture appearance was also measured, and the obtained values indicate almost no difference between the two materials. Furthermore, the values of T_o (the reference temperature) calculated from the fracture toughness measurements using the Master Curve methodology, also listed in Table 3, also confirm that these two steels are similar in the non-irradiated state.

4. Post irradiation examinations

To compare the effect of neutron irradiation on the properties of the investigated steels, both alloys were characterized in terms of microstructure, hardening and embrittlement.

Table 3
Transition temperatures obtained from Charpy and fracture toughness tests

Material	$DBTT_{KV}$ (°C)	$DBTT_{SFA}$ (°C)	T_o (°C)
T91	−71	−54	−113
E97	−58	−56	−115

4.1. Microstructure

The microstructure of irradiated T91 and EUROFER97 did not change after irradiation at 300 °C (as Eurofer was irradiated at this temperature only). However radiation induced defect clusters are present even after a low radiation dose of 0.06 dpa (Fig. 3(a) and (c)). The TEM images shown in Fig. 3 illustrates the microstructure of this two materials after irradiation to 0.06 dpa ((a) and (c)) and 1.5 dpa ((b) and (d)). The images have been taken with the same g and the same magnification to allow direct comparison. It can be readily seen that the size of the loops observed in EUROFER97 is substantially larger than for those found in T91. However, their number density seems to be similar as illustrated in Fig. 4. The defect density was calculated as n/V, where n is the number of defects counted in the image and V is the specimen volume at that location. The magnification of the microscope is calibrated and therefore the area can be measured directly. The local thickness of the specimen was determined by convergent beam electron diffraction. The defect density was measured on several locations and the average value is calculated. It can be noted that in the two steels the density of defects increases similarly with dose, but not the size. This effect is believed to be due to the difference in the binding energy between chemical elements such as Mo, Nb, Ni, etc., on one hand and W, Ta, V, etc., on the other hand, with the self-interstitial atoms in each of the steels [14].

4.2. Tensile tests

Tensile tests have been performed on irradiated specimens at a test temperature corresponding to the irradiation temperature. As

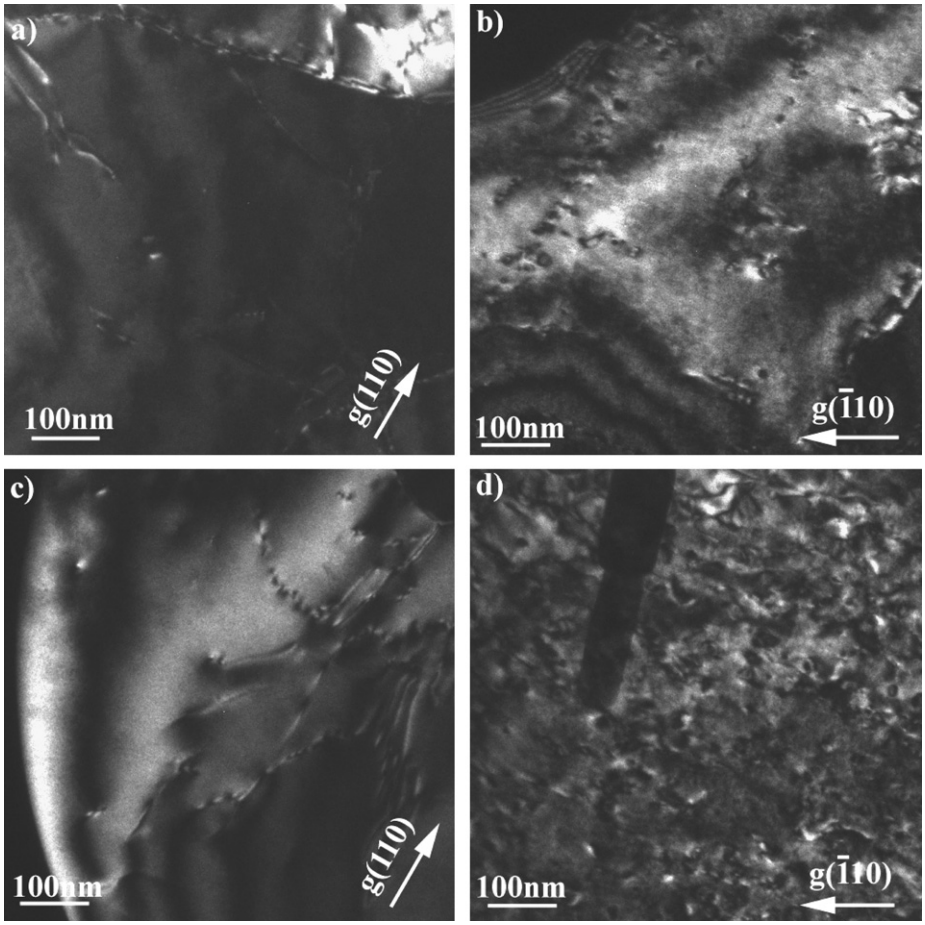

Fig. 3. Microstructure of irradiated T91 and E97: (a) T91 at 0.06 dpa, (b) T91 at 1.5 dpa, (c) EUROFER97 at 0.06 dpa and (d) EUROFER97 at 1.5 dpa.

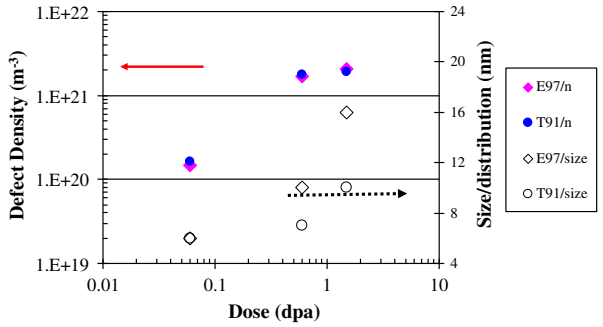

Fig. 4. Dose dependence of the defects density and size distribution of T91 and EUROFER97.

a consequence of irradiation, a substantial increase of yield and ultimate tensile strengths can be observed, as well as loss of ductility in both alloys. Fig. 5 shows the stress–strain curves for both materials before and after irradiation. Although both steels tested at 300 °C are showing the expected increasing strength and decreasing ductility with increasing irradiation dose, there are differences in the stress/strain response. Starting from 0.6 dpa, irradiation effects in EUROFER97 are more pronounced than in T91, showing a significant decrease in work hardening. Plastic instability in EUROFER97 occurring at this critical dose is even more pronounced for higher irradiation doses.

In terms of hardening, T91 appears to harden a little more than that of EUROFER97, particularly when the dose increases (Fig. 6). This small difference becomes more pronounced when the test temperature is lower than the irradiation temperature. Furthermore, Fig. 5 shows that the materials strongly differ in terms of flow behavior. T91, although showing more hardening, retains some work hardening or uniform elongation as illustrated in Fig. 7. On the other hand, EUROFER97 loses all its capacity to uniformly deform after irradiation but can still be plastically deformed (its total elongation is still significant, Fig. 7(left)). This behavior has already been observed in some other reduced activation ferritic/martensitc steels such as F82 [15] or in some conventional steels [16], especially after irradiation and testing at low temperatures. These type of tensile curves are caused by highly localised deformation and dislocation channeling [17]. However, the

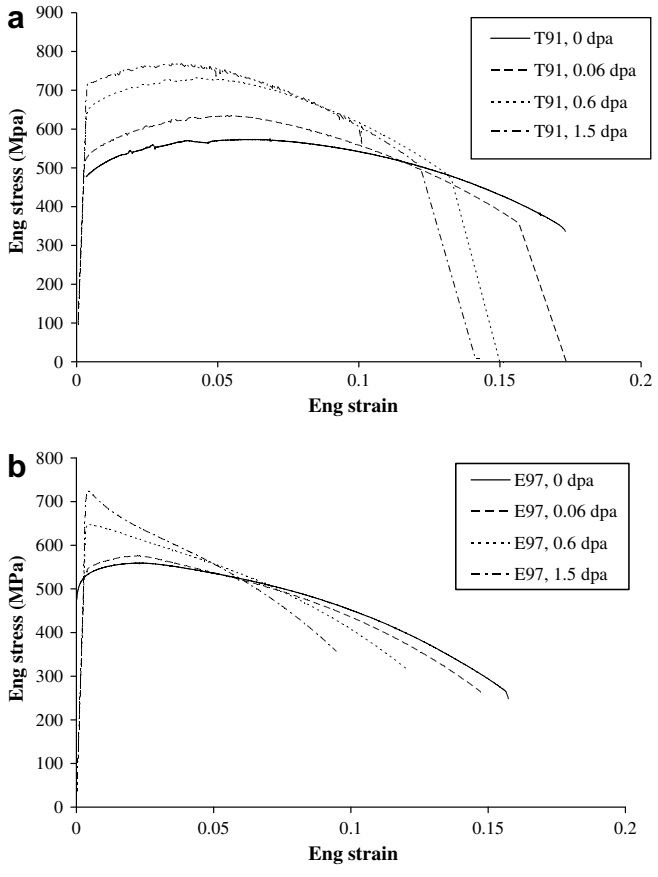

Fig. 5. Engineering stress–strain curves for: (a) T91 and (b) E97 at $T = 300$ °C for 0.06 dpa, 0.6 dpa and 1.5 dpa.

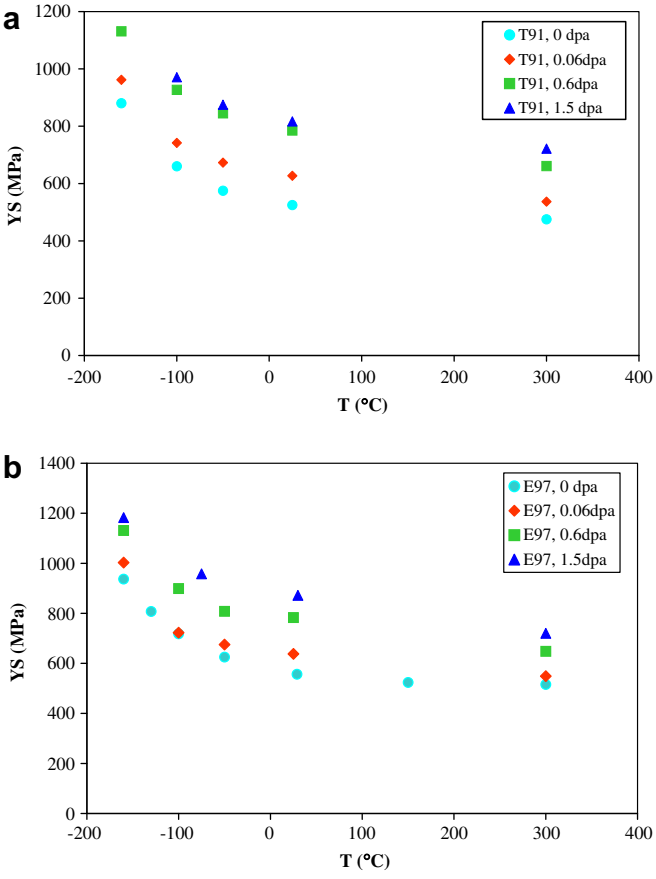

Fig. 6. Effect of testing temperature: yield strength dependence from temperature for: (a) T91 and (b) EUROFER97.

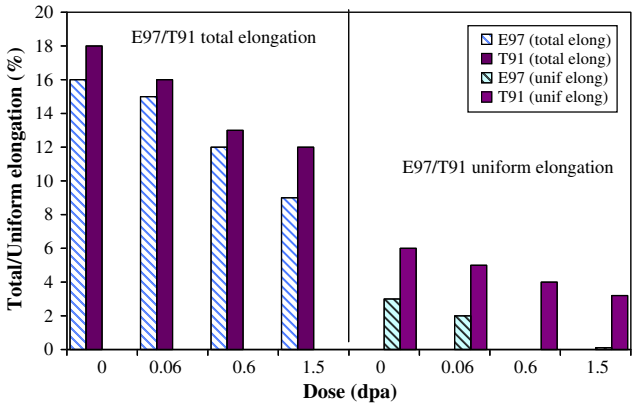

Fig. 7. Uniform/total elongation before and after irradiation at $T = T_{irr} = 300$ °C.

evidence of channeling in tempered martensitic steels is not so well established [18].

The fact that T91 does not present the same behavior as EUROFER97 is most probably due the distribution and size of the observed defects. In fact, irradiation induced-defects are much smaller in T91 than in EUROFER97 (Fig. 3), and their distribution appears to be more homogenous in T91 than in EUROFER97. We believe that the presence of big loops decorating the dislocation lines might play the precursor role for dislocation pile-ups which leads to localized deformation.

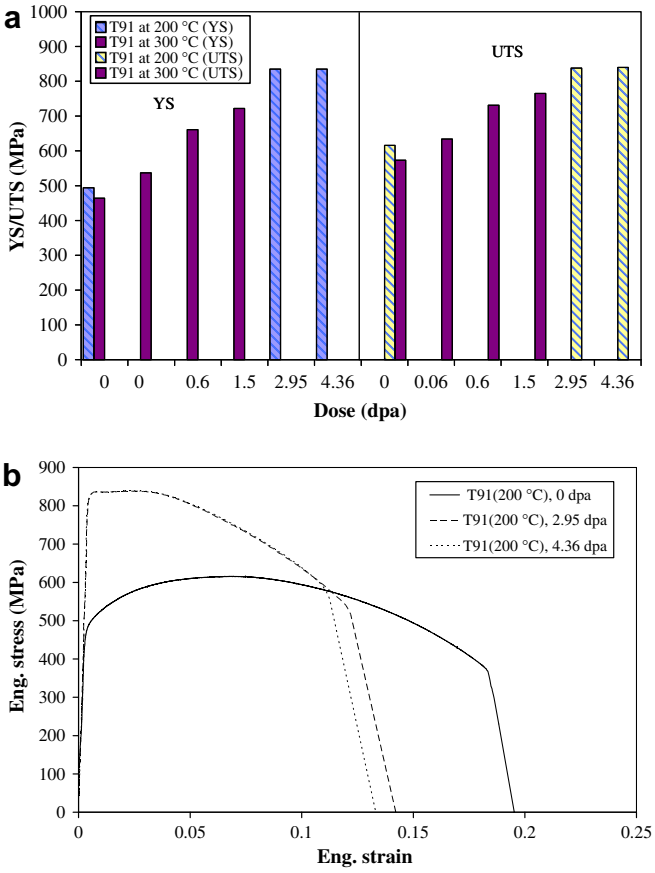

Fig. 8. (a) Temperature effect for T91 irradiated at 200 °C and 300 °C (yield and ultimate tensile strength dependence from the dose and uniform and total elongation dependence from the dose), (b) Engineering stress–strain curves for T91 irradiated at 200 °C.

As stated earlier, the localized deformation depends not only on the irradiation dose but also on the temperature [19]. It is much more pronounced at higher doses and lower temperatures. To verify this hypothesis, T91 has been irradiated at 200 °C to two doses (2.94 and 4.3 dpa). As can be seen from the stress–strain curves displayed in Fig. 8(b), although the hardening induced by this low temperature irradiation is much higher than the one induced by the irradiation at 300 °C (Fig. 5), the material still exhibits non-negligible hardening capacity in contrast to what has been observed in other Fe–Cr steels especially the low activation ones such as F82H [15].

4.3. Charpy and fracture toughness tests

Impact test results for T91 irradiated at 200 °C are shown in Fig. 9. The tests on the irradiated material have been performed between −30 °C and 200 °C (irradiation temperature) in order to establish full transition curves for absorbed energy and shear fracture appearance. Rather smooth transition slopes are observed in both unirradiated and irradiated conditions, with a pronounce irradiation shift and a decrease of USE that is limited to less than 10%. The small difference observed between the results observed at these two doses might be an indication that saturation of the defect density has been reached.

As far as fracture toughness tests are concerned, the Master Curve methodology was applied; this approach was originally developed for pressure vessel (RPV) steels [13]. For such materials, brittle fracture in the ductile to brittle transition regime is governed by the distribution of the cleavage initiators, which are randomly located in the material ahead of the crack tip. Such a distribution can be statistically treated using the weakest-link theory [20] associated with a three parameter Weibull distribution of fracture toughness values. For this reason, according to the standard the MC method cannot be used more than 50 °C below the reference temperature, where fracture is no more

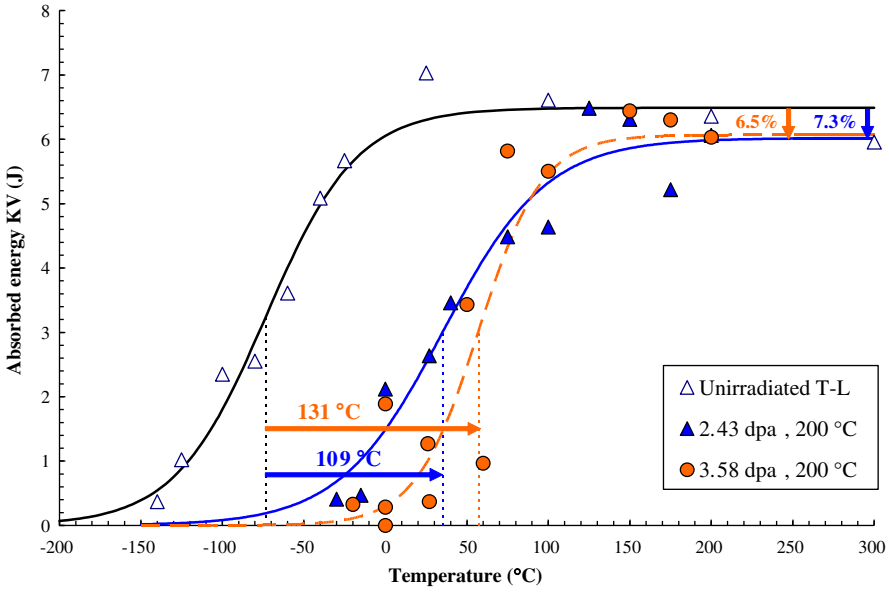

Fig. 9. Absorbed energy values obtained from unirradiated and irradiated T91 at 200 °C.

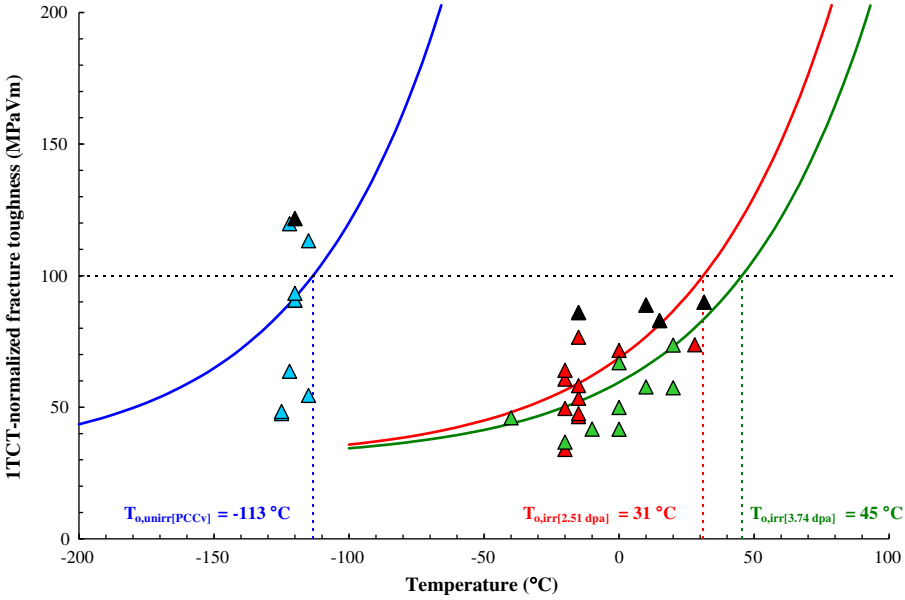

Fig. 10. Fracture toughness tests results for T91 after irradiation at 200 °C.

triggered by individual initiation sites. An upper limit on K_{Jc} values is imposed to ensure sufficiently high constraint conditions along the crack front at fracture. This limit is meant to guarantee that a single parameter adequately describes the crack-front deformation state [21]. When cleavage fracture is preceded by excessive ductile crack growth, fracture becomes strain-controlled rather than stress-controlled. Fig. 10 shows the 1T-normalised fracture toughness as a function of test temperature together with the corresponding Master Curves obtained for unirradiated and irradiated T91. The data obtained from the Charpy impact tests when considering dial energy or shear fracture appearance, and those obtained from the fracture toughness tests are listed in Table 4, together with results obtained from tests performed on EUROFER97 [22].

Two remarks can be formulated:

(1) The ductile to brittle transition temperature shifts obtained on EUROFER97 are much smaller than for T91. This indicates that EUROFER97 is more resistant to irradiation-induced embrittlement than T91, despite the absence of uniform elongation at the same doses.
(2) The shifts obtained from fracture toughness tests are significantly higher than those measured from impact tests. Fig. 11, where a comparison between T_o and DBTT shifts is shown for ferritic/martensitic steels and RPV steels, shows that the Charpy results are systematically non-conservative for the former class of materials [23].

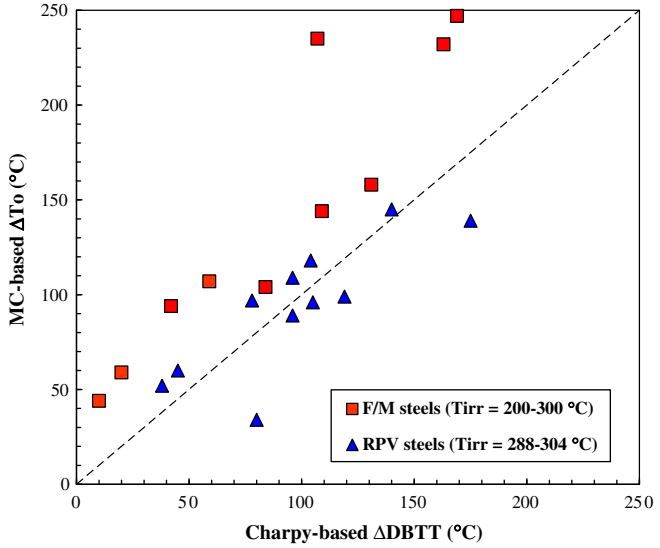

Fig. 11. Comparison between irradiation-induced shifts of DBTT and T_o.

Table 4
Irradiation-induced shifts of DBTT obtained from Charpy and fracture toughness tests on T91 irradiated at 200 °C and EUROFER97 irradiated at 300 °C

Material	T_{irr} (°C)	Dose (dpa)	$\Delta DBTT_{KV}$ (°C)	$\Delta DBTT_{SFA}$ (°C)	ΔT_o (°C)
T91	200	2.51	109	123	159
T91	200	3.74	131	120	145
E97	300	0.34	49.1	40.2	62.1
E97	300	0.71	39	29.4	47.7
E97	300	1.5	10.1	10.7	14.5

5. Conclusions

EUROFER97, an experimental reduced activation ferritic/martensitic steel developed within the European Fusion development agreement (EFDA), has been characterized, irradiated, tested and compared to the conventional ferritic/martensitic steel T91. It was found that, although the initial microstructure of both steels is quite similar in the as-received condition, they behave quite differently after irradiation. T91 hardens more than EUROFER97 when irradiated under the same conditions, but retains a significant amount of uniform elongation. It is stated that both the size and the distribution of the irradiation induced dislocation loops are the responsible for this difference. However, the shift of the DBTT is more moderate in EUROFER97 than in T91, indicating that the former is more resistant to embrittlement than the latter. Another important remark is that the Charpy impact tests should be considered as non-conservative when assessing the performance of ferritic/martensitic steels after irradiation.

Acknowledgements

The authors would like to acknowledge their colleagues of the mechanical and microstructure groups of the Institute of Nuclear Material Science in Mol, for their assistance and help during the experiments, and also the Technology department for the fabrication of the irradiation rigs. This work has benefited a lot from the stimulating discussions and encouragements received from Drs L. Malerba, W. van Renterghem and M. Decréton.

This work was partially funded by the European Fusion Development Agreement under the TTMS-007 task.

References

[1] L.K. Mansur, A.F. Rowcliffe, R.K. Nanstad, S.J. Zinkle, W.R. Corwin, R.E. Stoller, J. Nucl. Mater. 329–333 (2004) 166.
[2] H. Ait Abderrahim, D. De Bruyn (Eds.), MYRRHA Pre-Design File – Draft 2, Report R-4234, Studiecentrum voor Kernenergie – Centre d'Etude de l'Energie Nucléaire, 2005, Belgium.
[3] R.L. Klueh, D.R. Harries, High-Chromium Ferritic and Martensitic Steels for Nuclear Applications, ASTM, 2001.
[4] A. Alamo, M. Horsten, X. Averty, E.I. Materna-Morris, M. Reith, J.C. Brachet, J. Nucl. Mater. 283–287 (2000) 353.
[5] R. Lindau, A. Möslang, M. Schirra, Fus. Eng. Des. 61&62 (2002) 659.
[6] S.A. Maloy, M.B. Toloczko, K.J. McClellan, T. Romero, Y. Kohno, F.A. Garner, R.J. Kurtz, A. Kimura, J. Nucl. Mater. 356 (2006) 62.
[7] P. Dubuisson, D. Gilbon, J.L. Séran, J. Nucl. Mater. 205 (1993) 178.
[8] A. Alamo, J.L. Bertin, V.K. Shamardin, P. Wident, J. Nucl. Mater. 367–370 (2007) 54.
[9] T. Yamamoto, G.R. Odette, H. Kishimoto, J.W. Rensman, P. Miao, J. Nucl. Mater. 356 (2006) 27.
[10] P. Patriarca, S.D. Harkness, J.M. Duke, L.R. Cooper, Nucl. Technol. 28 (1976) 516.
[11] H. Schneider, Foundary Trades J. 108 (1960) 562.
[12] M. Weber, MIRE-CR-irradiation Report NT.57/F040112/0/MW/MM/AA.rw, SCK-CEN Internal Report, 2004.
[13] E. Lucon, A. Almazouzi, Mechanical response to irradiation for three high-Cr martensitic steels (EM10, T91, HT9)-Final Report: specimens irradiated to 2.6 and 3.6 dpa, SCK•CEN Report BLG-986, 2004.
[14] M. Matijasevic, A. Almazouzi, Effect of the chemical composition on the mechanical and microstructural behaviour of Fe–9Cr of ferritic/martensitic steels after n-irradiation at 300 °C, submitted for publication.
[15] A.F. Rowcliffe, J.P. Robertson, R.L. Klueh, K. Shiba, D.J. Alexander, M.L. Grossbeck, S. Jitsukawa, J. Nucl. Mater. 258–263 (1998) 1275.
[16] R.L. Klueh, J.M. Vittek, M.L. Grossbeck, J. Nucl. Mater. 103&104 (1981) 1275.
[17] A.L. Bement, in: Proceedings of ICSMA 2, vol. 2. Asilomar CA, 1970, p. 693.
[18] N. Hashimoto, R.L. Klueh, M. Ando, H. Tanigawa, T. Sawai, R. Shiba, Fus. Sci. Technol. 44 (2006) 490.
[19] R.E. Clausing, L. Heatherly, R.G. Faulkner, A.F. Rowcliffe, K. Farrel, J. Nucl. Mater. 141–143 (1986) 978.
[20] T.L. Anderson, D. Steinstra, R.H. Dodds, Fracture Mechanics, vol. 24, ASTM STP 1207, ASTM, 1994, p. 185.
[21] C. Ruggeri, R.H. Dodds, K. Wallin, Eng. Fract. Mech. 60 (1) (1998) 19.
[22] E. Lucon, Mechanical properties of the European reference RAFM steel (EUROFER 97) before and after irradiation at 300 °C (0.3–2 dpa), SCK-CEN Report BLG-962, 2003.
[23] E. Lucon, J. Nucl. Mater. 367–370 (2007) 575.